Modeling and Analysis of Hysteresis Phenomena in Electrostatic Zipper Actuators

P. Guidotti* and D. Bernstein**

* Applied Mathematics 217-50, Caltech, Pasadena, CA, gpatrick@its.caltech.edu
** MEMSCAP Inc., 180 Grand Ave., Oakland, CA, David.Bernstein@memscap.com

ABSTRACT

We investigate the relationship between the pull-in phenomenon for electrostatic actuators and the hysteresis effect found in zipper actuators. Like lumped mass and spring and tension based membrane models, we show that a beam model of a simple electrostatic actuator device has a fold and a corresponding pull-in voltage. When a dielectric layer is added to the model, however, the fold disappears for certain values of the dielectric constant and layer thickness. We use a variational formulation of the model to compute the location of the zipped states and show that the disappearance of the fold corresponds to the disappearance of the hysteresis effect in the zipper actuator. Hence the existence of the fold, and of the corresponding unstable state, is crucial for understanding the hysteresis observed in previous studies of zipper actuators.

Keywords: Electrostatic, Actuator, MEMS, Hysteresis, Pull-in

1 INTRODUCTION

It is well known that electrostatically actuated MEMS devices show a pull-in instability due to the impossibility of balancing the nonlinearly growing electrostatic force with elasticity. The lumped mass and spring model studied in [1], [2], [11], [3] can be used, as a first approximation, to explain the phenomenon. For each value of the applied voltage less than the pull-in voltage this model has three solutions: two physical states lying above the ground plate, one stable and one unstable, and an unphysical state lying below the ground plate. In [8] it was shown that the existence of the unstable state is not relegated to simple, zero dimensional models of this type, but rather may be a generic phenomena applying to all electrostatic actuators.

In this paper we extend the analysis contained in [8] in three ways: Firstly, we model the actuator with a more realistic beam model which also has two solutions before pull-in, one stable and the other not. Secondly, we add a dielectric layer on top of the ground plate in order to model the pulled in states, which we refer to as "zipped" states after the zipper actuators discussed in [9], [10]. Thirdly, we take a variational approach and show that the non-zipped states are local extrema of an appropriate energy functional which also satisfy the beam equation.

The paper is organized as follows: In Section 2 we derive the model and determine the governing equation for a pure elasticity model with two types of boundary conditions. In Section 3 we introduce a variational formulation of all three models and describe how it can be used to give a detailed mathematical analysis of the two beam models. A summary of the analysis is presented. We show that the zipped states are energy minimizing states which don't satisfy the beam equation but only a variational inequality. We also show that for certain geometries the fold disappears from the solution space of the model and as a consequence the hysteresis effect also disappears. Hence we conclude that the existence of the unstable state is necessary for the hysteresis effect. In Section 4 we present some results which have been numerically computed using the code AUTO. A summary of the results is given in Section 6.

2 THE MODEL

We consider a thin beam suspended above a rigid plate. The beam is assumed to be of rectangular shape, of width W, length L, and of negligible thickness. The beam and ground plate are assumed to be composed of a conducting material with a layer of insulating material of dielectric constant $\kappa\epsilon_0$ and thickness d on top of the ground plate. The dimensions of the ground plate are assumed to be much larger than that of the beam.

The ground plate is held at zero potential while a potential V is applied to the beam. With no applied potential the beam lies a distance l above the top of the insulating layer, hence the distance between the beam and the ground plate in this case is $l + d$. The model is illustrated in Figure 1.

We will consider two cases: one in which the beam is clamped on the two opposite edges of length W and free on the two remaining edges, and another in which the beam is clamped on only one such edge and free on the remaining three edges. Since we will explicitly neglect fringing effects in the solution of the electrostatic problem below, we assume that $W \gg L$.

We denote the coordinate system (see Figure 1) by (x', y', z'), the electrostatic potential by ϕ' and the deflection of the beam by u'. We work in the dimensionless

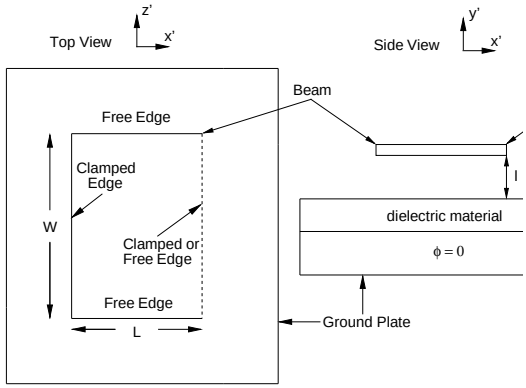

Figure 1: Model of electrostatically actuated device. The beam has length L and is separated from the ground plate by a distance l in the undeformed state.

variables

$$x = x'/L, \quad y = y'/l, \quad z = z'/W, \quad u = u'/l, \quad \phi = \phi'/V, \tag{1}$$

and in addition it will be convenient to define

$$\delta = \frac{d}{d+l} \text{ and } k = \frac{\delta}{\kappa(1-\delta)}. \tag{2}$$

Note that the origin of the unprimed coordinate system is such that lower surface of the undeflected beam is located at $y = 0$ and the left and right edges of beam at $x = \pm 1/2$. Hence, the upper surface of the dielectric is located at $y = -1$ while the ground plate is located at $y = -1 - d/l$.

The electrostatic potential ϕ' satisfies the Laplace equation in both the dielectric and free space regions. Neglecting the fringe fields on the edges of the beam this is

$$\epsilon^2 \frac{\partial^2 \phi}{\partial x^2} + \frac{\partial^2 \phi}{\partial y^2} = 0 \tag{3}$$

with boundary conditions

$$\phi(x, y = u) = V, \quad \phi(x, y = -1 - d/l) = 0. \tag{4}$$

Here $\epsilon = l/L$ is the aspect ratio of the device. Letting ϵ go to zero in the above and using the appropriate jump condition for the gradient of the potential at the surface of the dielectric gives

$$\phi = \frac{1 + y + k}{1 + u + k}. \tag{5}$$

The displacement u' is assumed to satisfy (see, e.g., [5], [4], [6], [7])

$$EI \frac{\partial^4 u'}{\partial x'^4} - T \frac{\partial^2 u'}{\partial x'^2} = -\frac{1}{8\pi} |\nabla \phi'|^2. \tag{6}$$

Here E is the effective Young's modulus of the beam, I its second moment of inertia, and T a tensile force applied to the beam. In this paper we will only consider tension free models and hence set $T = 0$ from here on. For the right hand side of (6) we have

$$|\nabla \phi'|^2 = \frac{V^2}{l^2} \left(\epsilon^2 (\frac{\partial \phi}{\partial x})^2 + (\frac{\partial \phi}{\partial y})^2 \right). \tag{7}$$

Again neglecting the ϵ^2 term, this reduces to

$$|\nabla \phi'|^2 \approx -\frac{1}{8\pi} \frac{V^2}{l^2} \frac{1}{(1+u+k)^2}. \tag{8}$$

Hence the governing equation for the model is

$$u_{xxxx} = -\frac{\beta}{(1+u+k)^2} \tag{9}$$

where the dimensionless parameter β is defined by $\beta = V^2 L^4 / (8\pi E I l^3)$.

We may choose one or both of the edges located at $x = \pm 1/2$ to be clamped. We choose not to investigate pinned beams. The clamped-clamped boundary conditions we will use are

$$u(-1/2) = u_x(-1/2) = 0, \quad u(1/2) = u_x(1/2) = 0. \tag{10}$$

while in the clamped-free case we have

$$u(-1/2) = u_x(-1/2) = 0, \quad u_{xx}(1/2) = u_{xxx}(1/2) = 0. \tag{11}$$

Note that we must distinguish between the parameter β for each set of boundary conditions. In what follows below we will also consider the "zipped" state boundary conditions

$$u(-1/2) = u_x(-1/2) = 0, \quad u(a) = -1, \quad u_x(a) = 0 \tag{12}$$

where $-1/2 < a < 1/2$.

3 ANALYSIS

As we have seen in the previous section, steady beam configurations correspond to solutions of a fourth order boundary value problem for the displacement. As in the membrane model studied in [8] this equation has a non-trivial bifurcation diagram. In the case in which $k = 0$ (which happens if either $d = 0$ or $\kappa \to \infty$) the bifurcation diagram, shown in Figure 2, contains a single fold so that there are two solutions for each value of β less than a critical value $\beta^* \approx 93$.

In the case $k > 0$ it is convenient to formulate the problem using a variational principle. An energy functional

$$E(u) = \int_{-1/2}^{1/2} \left((u_{xx})^2 - \frac{\beta}{1+u+k} \right) dx \tag{13}$$

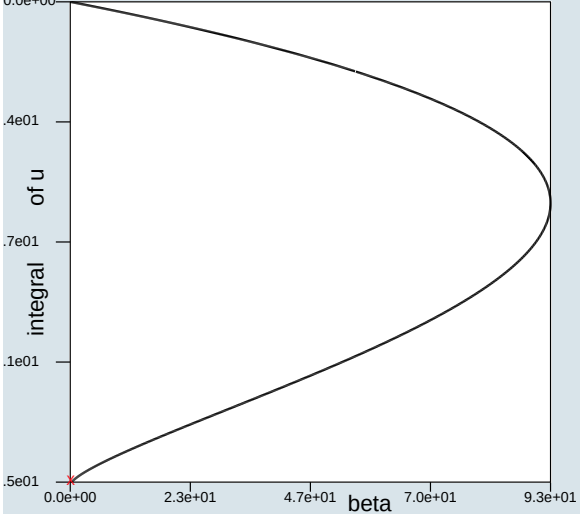

Figure 2: Bifurcation diagram for the beam problem with no insulating layer.

can be associated to the any beam configuration. The boundary value problem can be recovered from it as its Euler-Lagrange equation. It is obtained by taking its first variation in a space of configuration satisfying appropriate boundary condition. In the clamped-clamped case, solutions of the boundary value problem are critical points for E in the space of states satisfying all boundary conditions. In more mathematical words, u solves the boundary values problem if and only if u satisfies $u(j) = u_x(j) = 0\,,\ j = \pm 1/2$ and

$$\lim_{t\to 0} \frac{1}{t}\big(E(u + t\varphi) - E(u)\big) = 0 \tag{14}$$

for each smooth φ also satisfying the same boundary conditions. In the clamped-free case all states satisfying only the left boundary condition are allowed to compete and solutions of the boundary value problem correspond to critical points u of the energy functional (in the above sense) satisfying the left boundary condition $u(0) = u_x(0) = 0$. The functions φ are also only required to satisfy the left boundary condition. The other boundary condition is a natural one and is automatically satisfied by any critical point (if it is regular enough).

Now, taking this variational point of view doesn't give us any new information for non-insulated bottom plates ($k = 0$). Things change if we consider the insulated case. In fact the presence of the insulator can be mathematically modeled by adding the unilateral side condition that

$$u \geq -1 \tag{15}$$

to the variational problem for the energy functional. A critical point now only satisfies the boundary value problem if it happens to already lie completely above the insulator. Other critical points do however exist which are partly in contact with the insulator. In this case they cannot satisfy the boundary value problem. It therefore becomes essential to understand the bifurcation diagram for the energy functional itself. To do so we model the unilateral side condition by a penalty term in the energy functional

$$E_\varepsilon(u) = \int_{-1/2}^{1/2} \left((u_{xx})^2 - \frac{\beta}{1+u} + \frac{1}{\varepsilon}(-1-u)^+ \right) dx \tag{16}$$

where $(u)^+ = u$ if $u \geq 0$ and vanishes otherwise. The artificial parameter ε needs to be chosen small enough. After the introduction of the penalty term the unilateral condition need not be imposed any longer and the corresponding Euler-Lagrange equation can be derived. We obtain the modified boundary value problem

$$u_{xxxx} = -\frac{\beta}{(1+u+k)^2} + \frac{1}{\varepsilon} H(-1-u) \tag{17}$$

which has to be complemented with the appropriate boundary conditions for the considered cases. The function H is only different from zero for positive arguments where it has value 1. In our numerical computation we shall approximate H by $H \approx 0.5 + \arctan(Ku)/\pi$ for a large constant K.

4 RESULTS

To produce the bifurcation diagrams we need in order to understand pull-in and hysteresis we used a very convenient numerical toolbox for computing bifurcation diagrams called AUTO. It relies on the well-known arclength continuation method which is a very convenient numerical scheme to go around folds in bifurcation diagrams (see, e.g., [8]). In Figure 3 we plot the bifurcation diagram for the energy functional E_ε for different thicknesses and dielectric constants of the insulating layer in the clamped-clamped case. If the parameter k is not too large we see two folds whereas for larger values of k no fold (hence no pull-in or hysteresis) is observed. In the latter case the top plate comes in contact with the insulator before pull-in can occur. When present, the second fold happens for a parameter value β_* at which the unstable solution, appeared after the first fold, comes into contact with the insulator and thus producing the first zipped state. The solutions on the branch following the second fold are therefore all zipped states. In figure 4 we show some of the solutions along the bifurcation diagram for $k = 0.2$. The diagram also predicts and estimates the hysteresis behavior. Zipped states first appear when β becomes larger than β^* and they persist until the value β_* is attained when turning the voltage back down again.

5 CONCLUSION

We presented an analysis of the electrostatic "zipper" actuators discussed in [9], [10]. Using a simple

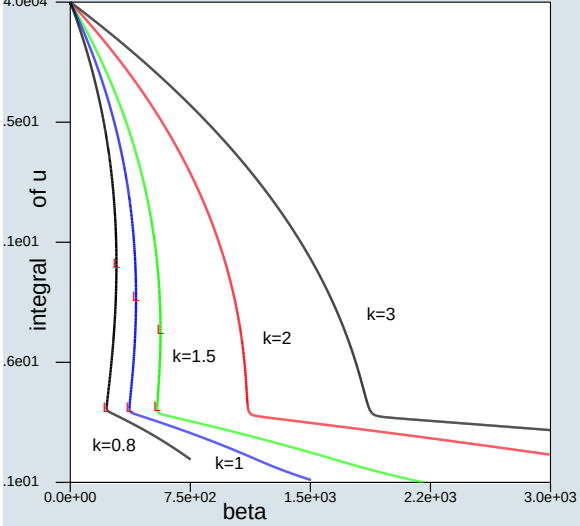

Figure 3: Bifurcation diagrams for the energy functional.

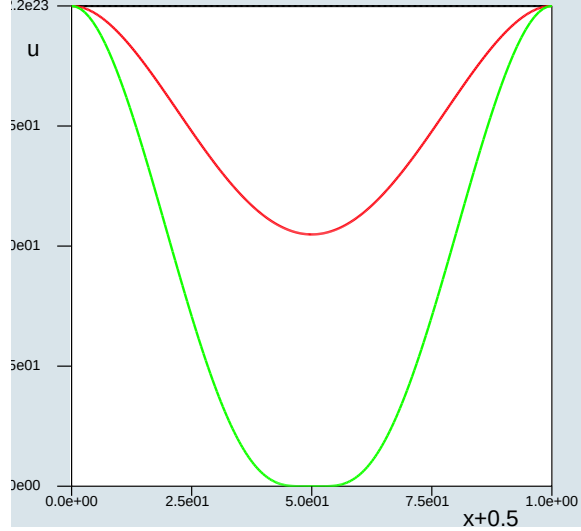

Figure 4: Typical solutions for $k = 0.2$. The figure depicts the solution at the first fold and a zipped state.

one dimensional model we showed that the hysteresis effect depends critically on the existence of an unstable stationary state and the corresponding fold in the bifurcation diagram of the underlying equation. In addition to obtaining useful existence and uniqueness (and non-uniqueness) results for the model, we showed that for certain combinations of geometry and dielectric constants the fold disappears from the solution space of the equation and as a consequence the hysteresis effect also disappears.

In order to account for the zipper effect, we extended the analysis contained in [8] in three ways: Firstly, we modeled the actuator with a more realistic beam model which, like the membrane model, has two solutions before pull-in, one stable and the other not. Secondly, we added a dielectric layer on top of the ground plate in order to model the pulled-in, or "zipped", states. Thirdly, we used a variational approach and showed that the non-zipped states are local extrema of an appropriate energy functional which also satisfy the beam equation. The zipped states are energy minimizing states which don't satisfy the beam equation but only a variational inequality.

REFERENCES

[1] H.C. Nathanson, W.E. Newell, R.A. Wickstrom and J.R. Davis, IEEE Trans. on Electron Devices 14 (1967), pp. 117-133.

[2] J.R. Gilbert, G.K. Ananthasuresh, and S.D. Senturia, Proceedings of the 9th Annual International Workshop on Micro Electro Mechanical Systems (1996), pp. 127-132.

[3] J.I. Seeger and S.B. Crary, in Proceedings of the 1997 International Conference on Solid-State Sensors and Actuators (1997), pp. 1133-1136.

[4] H.A.C. Tilmans and R. Legtenberg, Sens. Actuat. A 45 (1994), pp. 67–84.

[5] D. J. Ijntema and H. A. C. Tilmans, *Static and Dynamic Aspects of an Air-Gap Capacitor*, Sens. Actuat. A 35 (1992), pp. 121–128.

[6] M. J. Anderson, J. A. Hill, C. M. Fortunko, N. S. Dogan, and R. D. Moore, *BroadBand Electrostatic Transducers: Modeling and Experiments*, J. Acoust. Soc. Am. 97 (1995), pp. 262–272.

[7] E.S. Hung and S.D. Senturia, *Leveraged Bending for Full-Gap Positioning with Electrostatic Actuation*, Solid State Sensor and Actuator Workshop, 1998, Hilton Head, S.C., June 8-11, pp. 83-86.

[8] D. Bernstein, P. Guidotti, and J.A. Pelesko *Mathematical Analysis of Electrostatically Actuated MEMS Devices*, MSM2000 proceedings.

[9] J.R., Gilbert, G.K., Ananhasuresh, and S.D. Senturia, *3D Modeling of Contact Problems and Hysteresis in Coupled Electro-Mechanics*, Proceedings of 9th Annual International Workshop on Micro-Electro-Mechanical Systems, Feb 11-15, 1996, pp. 127-132.

[10] J.R. Gilbert and S.D. Senturia *Two-Phase Actuators: Stable Zipping Devices Withour Fabrication of Curved Surfaces*, Solid State Sensor and Actuator Workshop, 1996, Hilton Head S.C., pp. 98-100.

[11] F. Shi, P. Ramesh, and S. Mukherjee, *Simulation Methods for Micro-Electro-Mechanical Structures (MEMS) with Application to a Microtweezer*, Comp. Struct., 56 (1995), pp. 769–783.